

# Numerical Simulation of Rarefied Flow Instabilities Using Kinetic Approach

*Anton A. Shershnev*<sup>1</sup>, *Alexey N. Kudryavtsev*<sup>1</sup>, *Alexander V. Kashkovsky*<sup>1</sup>,  
*Semyon P. Borisov*<sup>1</sup>, *Sergey O. Poleshkin*<sup>1</sup>

© The Authors 2024. This paper is published with open access at SuperFri.org

The results of numerical investigations of hydrodynamic instabilities in rarefied flows obtained using the kinetic approach are presented and discussed. The rarefied flow instabilities are simulated using both statistical and deterministic methods to solve kinetic equations for the velocity distribution function. The Direct Simulation Monte Carlo method is employed for statistical modeling of rarefied flows while the deterministic methods used are high-order finite-difference schemes for solving the Boltzmann transport equation and model kinetic equations in a multidimensional phase space. Numerical solvers used for the simulations are run on multiple-GPU clusters using CUDA platform and MPI communication interface. The development of instabilities in compressible free shear flows such as a mixing layer between two parallel streams and a plane jet in a coflow is considered. The Rayleigh–Taylor and Richtmyer–Meshkov instabilities induced by external body forces are also simulated. The results of kinetic simulations are compared with data from the linear stability theory and Navier–Stokes computations and it is shown that good agreement is observed between kinetic and continuum approaches.

*Keywords:* DSMC method, the Boltzmann transport equation, model kinetic equations, mixing layer, plane jet, the Rayleigh–Taylor instability, the Richtmyer–Meshkov instability.

## Introduction

Fluid flow instabilities are a common physical phenomenon important for many problems in science and engineering. They are usually considered on the basis of the continuum approach since they happen at high Reynolds numbers and, therefore, low Knudsen numbers. However, in several important cases, flow instabilities may emerge in conditions when the effects of flow rarefaction are pronounced. Those cases include, for example, instabilities associated with the action of mass forces (gravity force in the Rayleigh–Taylor instability and Rayleigh–Benard convection, inertial force in the Richtmyer–Meshkov instability). Flow instabilities may also emerge at low Reynolds numbers in free shear flows (mixing layers, jets and wakes), flows with curved streamlines (such as the Taylor–Couette flow) and, as an extreme case, in a collisionless medium with long-range forces. Rarefaction effects may become noticeable at instability of high-speed flows. Numerical simulation of such phenomena demands a step beyond the standard continuum approach based on the Navier–Stokes equations and should be based on the molecular-kinetic description taking into account atomistic structure of matter.

There is a number of kinetic approaches that can be used for this purpose: the Molecular Dynamics (MD), the Direct Monte Carlo Simulation (DSMC), finite-difference methods that solve the Boltzmann transport equation or its simplified versions, the so-called model kinetic equations, on a grid in a multidimensional phase space. Since 1980s the MD and the DSMC were applied to the simulation of the “stability switch” in problems of convection in the planar layer of gas [1–4], and formation of the Taylor vortices in the cylindrical Couette flow [5–7]. The stability switch means that, as a result of an instability, one steady flow is replaced by another but also steady flow (“secondary flow”). Slightly later the stationary Taylor–Görtler longitudinal vortices

---

<sup>1</sup>Khristianovich Institute of Theoretical and Applied Mechanics Siberian Branch of Russian Academy of Sciences, Novosibirsk, Russian Federation

in the curved mixing layer of a supersonic underexpanded jet were simulated by directly solving the Boltzmann equation in the 6D phase space [8, 9].

However, in general, the instability development is connected with time dependent disturbances. Even if a steady secondary flow forms, unsteady processes will dominate in later stages of the instability leading finally to transition to turbulence. Kinetic simulations of such complicated unsteady phenomena require a huge amount of computer resources. It seems that the first time-accurate kinetic simulation of a flow instability was performed in [10] where early stages of the Kelvin–Helmholtz instability were simulated by solving the model kinetic equations.

In recent years, with increasing computer power, numerical investigation of flow instabilities on the kinetic level has become an actively developing research field. Rarefied flow instabilities were simulated using the MD [11, 12], the DSMC method [13–19] and deterministic solution of model kinetic equations or, even, the Boltzmann transport equation [20–22].

In the current paper, we overview and discuss the results of numerical investigations of hydrodynamic instabilities in rarefied flows obtained in recent years in Laboratory of Computational Aerodynamics at Khristianovich Institute of Theoretical and Applied Mechanics, Novosibirsk (ITAM SB RAS). The numerical simulations have been performed with a number of numerical kinetic techniques including both the statistical DSMC method and deterministic approaches for solving kinetic equations in the multidimensional phase space. Navier–Stokes computations have been undertaken for comparison and, sometimes, for parametric investigation.

All numerical codes used for these simulations are developed in the Laboratory and designed for massive parallel computations on hybrid (GPU/CPU) computational clusters employing, for parallelization, NVIDIA CUDA platform and MPI communication interface.

The problems simulated include instabilities of high-speed free shear flows – the Kelvin–Helmholtz instability of a supersonic mixing layer, the instabilities developing in supersonic plane jets with co-flow, the instabilities driven by body forces – the Rayleigh–Taylor instability of the interface between heavier and lighter gases in a gravitational field, the Richtmyer–Meshkov instability developing on a contact surface after passing a shock wave. The instabilities in gravitating collisionless media such as those presented in [23] are out of scope of this paper.

The remainder of the paper is organized as follows. In Section 1 the numerical solvers and parallelization techniques used are reviewed. The results of numerical simulations of rarefied flow instabilities are presented and discussed in Section 2. The study is briefly summarized in Conclusion.

## 1. Solvers and Parallelization Techniques

In this section a brief description of the solvers used for the numerical simulations is presented. Although each solver is based on the different set of equations, they all are developed using the same paradigm. The codes are written in C++ and use CUDA API to perform computations on GPUs. The domain decomposition technique is employed for parallelization and data exchange between processors is performed via MPI library. Some details on code implementation are given below.

### 1.1. Direct Simulation Monte Carlo Solver

Software systems of the SMILE family, namely SMILE++ and SMILE-GPU, are used in the DSMC simulations. The former is a well-established numerical code which takes most of the ad-

vantages of object-oriented programming including inheritance and encapsulation, and contains a large variety of physical models [24]. It is based on the efficient majorant frequency scheme for collisions and uses a nested octree-like Cartesian computational grid. Since the DSMC is a particle-based method, the computational load depends directly on the number of model particles in the simulation, conventional domain decomposition does not allow to divide the computational load evenly. In the case of the SMILE++ code this problem is treated by distributing computational cells randomly across the CPUs, which yields relatively balanced computational times and a good parallelization efficiency.

The SMILE-GPU code [25] is a high-performance version of the DSMC solver specifically for hybrid architectures and is designed for large 3D computations. Computations on multiple GPUs are performed using the domain decomposition approach along with adaptive load balancing. In accordance with Direct Timing Load Balance algorithm [25], computational *cells* are periodically (usually every 1000 time steps) redistributed between GPUs depending on the average wall clock time spent by each GPU on the one iteration. The smaller the time of computation on a certain GPU the more additional cells will be assigned to it at the next load balance correction. Usually after 10–20 iterations of balance corrections it yields approximately 95–99% efficiency. It should be noted that this algorithm works quite well even for unsteady flows.

## 1.2. Solver for Boltzmann and Model Kinetic Equations

Another computational code used for numerical simulation of rarefied flow instabilities is based on finite-difference methods for kinetic equations governing the evolution of the particle velocity distribution function. The code employs the method of discrete ordinates in the velocity space and high-order TVD and WENO schemes for the spatial approximation. Intermolecular collisions are taken into account using either the full multidimensional Boltzmann collision integral or a simplified relaxation-type term. In the former case, the collision integral is evaluated using the numerical techniques described in [26, 27]. In the latter case, the relaxation-type term can be taken in the form corresponding to the BGK equation [28], the statistical ellipsoidal model [29] or the Shakhov model [30]. The composite Simpson rule or the Gauss–Hermite quadratures are used to evaluate integrals in the velocity space [31]).

The code is written in C++ programming language and implements CUDA API and MPI library to run simulations on multiple GPUs. Decomposition of the computational domain in the physical space is used to distribute the load between processor units [27].

## 1.3. Navier–Stokes Solver

To compare results of kinetic and continuum simulations, some Navier–Stokes computations have also been performed. In these cases, the HyCFS-R solver for compressible flows of gas mixtures [32] is used. The Navier–Stokes equations in general curvilinear coordinates are solved on a multiblock structured grid using TVD and WENO shock-capturing schemes for spatial discretization and Runge–Kutta TVD schemes for time advancement. The code is primarily designed for hybrid CPU/GPU computational environments and its multilevel parallelization is based on the domain decomposition used with CUDA API, OpenMP API and MPI protocol. The domain is divided into separate partitions, each partition is assigned to a specific GPU and then inter-partition exchange is carried out using either OpenMP if both blocks are located on the same computational node, or using MPI library otherwise.

## 2. Results of Numerical Simulations

### 2.1. Kelvin–Helmholtz Instability in a Mixing Layer

A mixing layer between two parallel streams can be considered as a prototype of all free shear flows such as jets and wakes. The Kelvin–Helmholtz (KH) instability [33] is the dominant instability mechanism in the mixing layer at low convective Mach numbers  $M_c = (U_1 - U_2)/(a_1 + a_2)$ , where  $U_1, U_2$  are the velocities of two streams and  $a_1, a_2$  are speeds of sounds in them. The mixing layer is subject to the KH instability even at low Reynolds numbers.

The KH instability can be simulated as developing either in time or in space. In the former case the flow is assumed to be periodic along the streamwise coordinate so that the mean flow and disturbances evolve in time. In the latter case they develop spatially; this formulation is closer to practice but more difficult to simulate numerically because it requires a much longer computational domain.

Numerical simulations based on the kinetic approach are performed in both formulations. DSMC simulations of the mixing layer are considered in the companion paper [34].

When the flow is simulated by solving the model kinetic equations, a computational grid in 4D (2 physical coordinate and 2 velocity components) phase space is used. It has been shown [31] that for low-speed flows the Gauss–Hermite quadratures are particularly efficient for evaluation of integrals in the velocity space. Numerical tests showed that the grid of  $11 \times 11$  points in the velocity space ensures integration of the initial flowfield with machine accuracy when the temporal mixing layer is simulated at the convective Mach number  $M_c = 0.2$  by solving the BGK equation.

In these simulations, the mean flow velocity is taken as  $U(y) = \tanh(y)$ , the temperatures of two streams are assumed to be equal,  $T_1 = T_2$ . An initial perturbation imposed on the mean flow is a superposition of the fundamental harmonic (most unstable disturbance in accordance with the linear stability theory) and its first and second subharmonics. The initial amplitudes of the subharmonics are much smaller than that of the fundamental harmonic.

The main stages of the instability development include the initial growth and saturation of the most unstable disturbance, the growth of the first subharmonic via the subharmonic resonance mechanism, then the growth of the second subharmonic. The fast growth of two subharmonics looks in the physical space as two successive vortex pairings. The process of vortex pairing reproduced on the grid of  $200 \times 200$  points in the coordinate space is shown in Fig. 1.

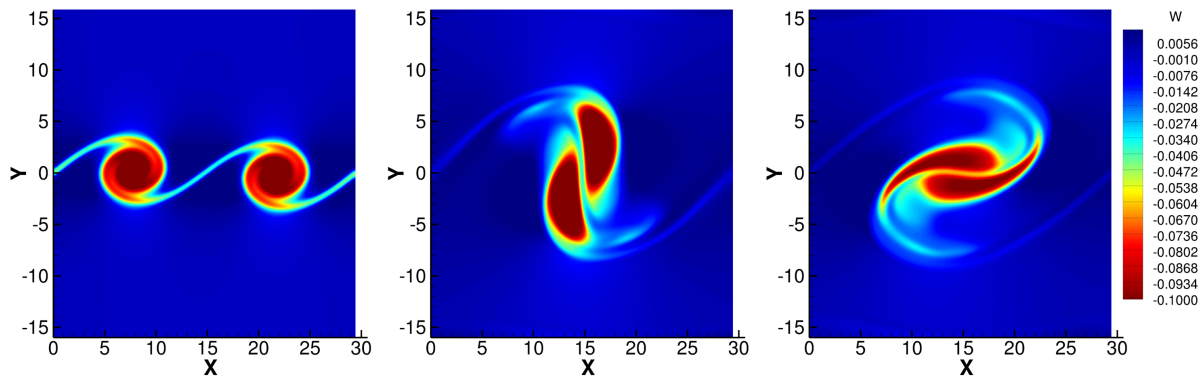


**Figure 1.** Vortex pairing in numerical simulation of the KH instability using the BGK kinetic equation. Vorticity flowfields in three time moments.  $M_c = 0.2$ ,  $T_2/T_1 = 1$

Figure 2a shows the time evolution of energies of the fundamental harmonic and two subharmonics with the wave numbers  $\alpha$ ,  $\alpha/2$  and  $\alpha/4$ , respectively. As a result of the subharmonic resonance [35], the energy is pumped, first, from the fundamental harmonics to its subharmonic and, then, from the first subharmonics to the second one. In the physical space it looks like successive vortex pairings.

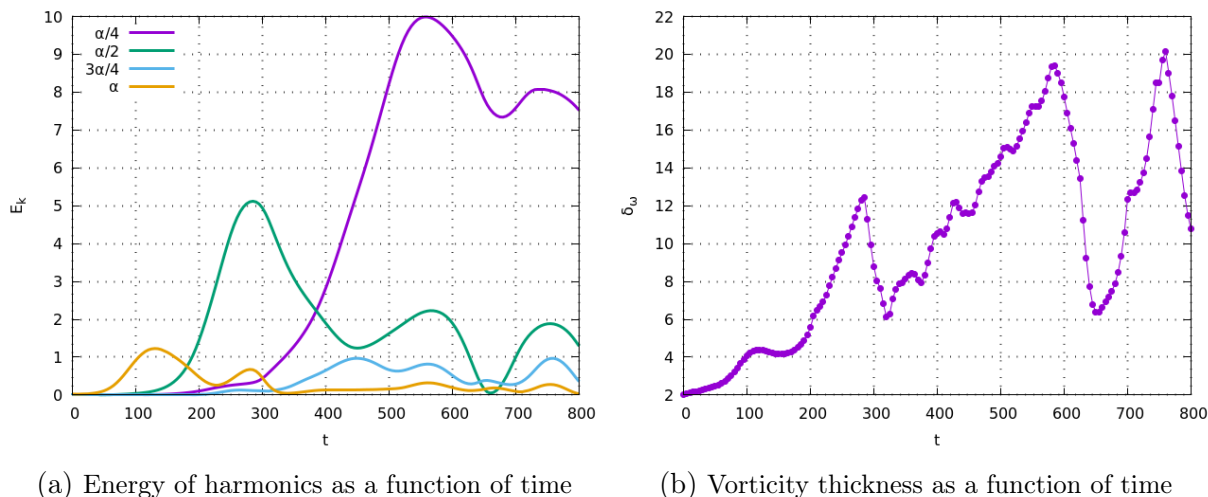


**Figure 2.** Time evolution of the supersonic mixing layer

Figure 2b shows the so-called vorticity thickness  $\delta_\omega = (U_1 - U_1)/(\partial U/\partial y)_{\max}$  as a function of time. The peaks at  $t \approx 290$ ,  $590$  and  $750$  correspond to the time moments when interacting pairs of neighboring vortices roll up around one another. Immediately after the vortex mergings the vorticity thickness abruptly drops.

The kinetic simulation successfully reproduces all stages of the KH instability development preceding the onset of 3D instability and transition to turbulence.

## 2.2. Instability of Supersonic Plane Jets in Coflow

A plane jet is another free shear flow unstable even at low Reynolds numbers. The linear theory predicts [36] that, at subsonic convective Mach numbers, there are two unstable modes of disturbances, the varicose (symmetric) mode and the sinuous (antisymmetric) mode. At higher supersonic  $M_c$  there appear multiple new unstable modes connected with resonant reflection of disturbances from the mixing layers bounding the jet. As a rule, the sinuous mode is the most unstable one.

Two different cases are considered with the jet Mach numbers  $M_j = 2.5$  and  $4.5$ . In both cases there is a parallel external coflow with the Mach number  $M_a = 1.5$ . The jet and coflow temperatures are the same, so that the convective Mach numbers are equal to  $0.5$  and  $1.5$ , respectively. The Knudsen number based on the jet width at the inflow and the mean free path in the coflow is  $0.0058$  in both cases.

The numerical simulations presented here are performed using the DSMC method. No initial perturbations are imposed on the mean flow because it can be expected that flow disturbances will develop from statistical fluctuations always present in DSMC simulations.

The SMILE-GPU code running on a computational cluster equipped with Nvidia Tesla V100 GPUs is employed for these simulations. For  $M_j = 2.5$  the total number of test particles is  $2 \cdot 10^9$

and the computation is performed on 12 GPUs. The wall-clock time per iteration is equal to 0.7 seconds. The corresponding figures for the  $M_j = 4.5$  case are  $10^9$  test particles, 8 GPUs and 0.5 seconds.

The computed flowfields sampled on the grid of  $1000 \times 400$  cells and averaged over a small time interval (equal to 200 time steps) are virtually indistinguishable from the results of Navier–Stokes simulations. As predicted by the linear stability theory, the sinuous mode of instability develops quite rapidly at the subsonic convective Mach number  $M_c = 0.5$ , see Fig. 3. Vortex interactions and pairings are observed at early stages of the instability development. The mean velocity profiles show that the jet mixing layers spread and meet one another, after that the centerline velocity starts to decrease while the jet width grows. Near the outflow boundary, the velocity on the jet axis reduces by about 1.5 times, and the mean velocity profile takes a characteristic “bell-like” shape, typical for a developed jet flow.

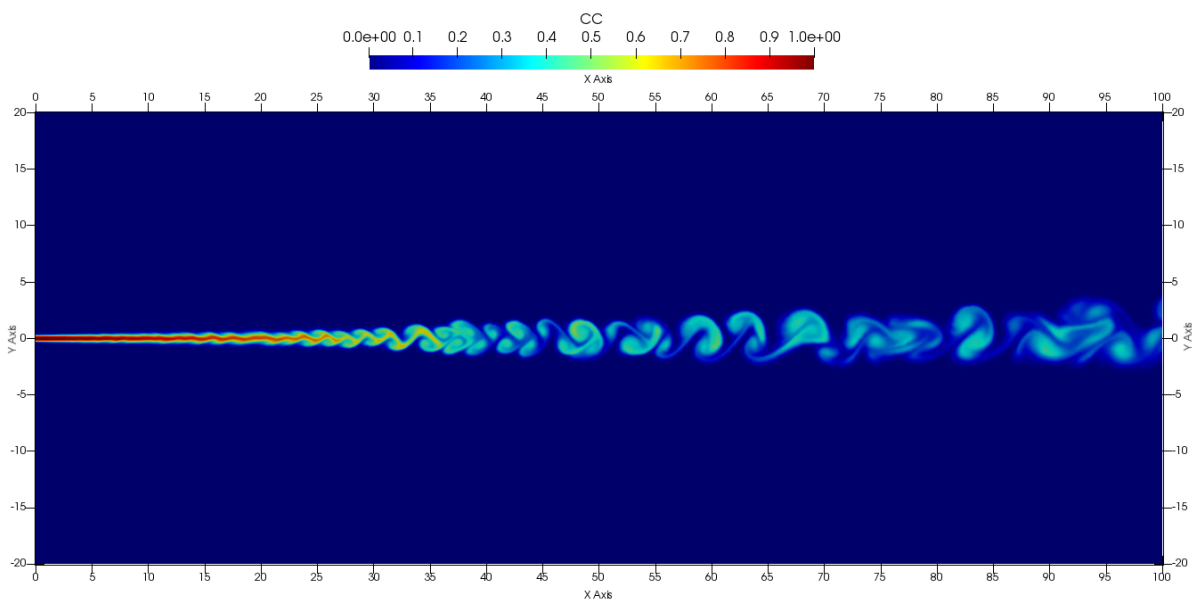


**Figure 3.** Plane jet instability. Flowfield of concentration of particles issuing from the nozzle.  
 $M_j = 2.5$ ,  $M_a = 1.5$

The antisymmetric mode also dominates at the supersonic convective Mach number  $M_c = 1.5$ , see Fig. 4. The vortex structures forming in this case are larger in size, and the breakdown of the jet column occurs at shorter distances from the nozzle exit. Weak oblique shock waves radiated from the jet are generated by the vortex structures moving with a supersonic speed relative to the external coflow.

Due to inherently stochastic excitation the flow instability develops more naturally in DSMC simulations than in computations with imposed artificial disturbances based on the deterministic approach. Thus, locations of successive vortex pairings are not fixed but scatter over some interval, so that the time-average jet width monotonically increases with the distance and does not include such abrupt peaks and drops as in Fig. 2b.

### 2.3. Rayleigh–Taylor Instability

The Rayleigh–Taylor (RT) instability occurs when a heavier fluid in a gravitational field is located above a lighter fluid. It is observed in a wide variety of natural phenomena and technical

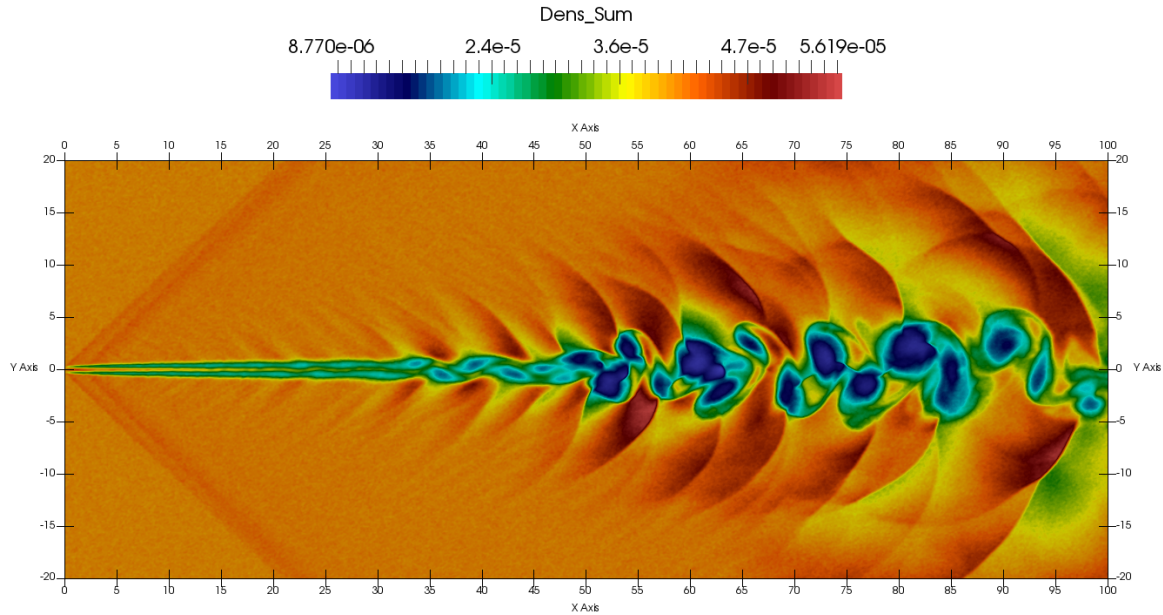


**Figure 4.** Plane jet instability. Density flowfield.  $M_j = 4.5$ ,  $M_a = 1.5$

applications, from supernova explosions and accretion of matter on black holes to inertial fusion, the formation of oddly shaped clouds and the flow of liquid from an inverted glass. The RT instability has been investigated in many theoretical, experimental, and numerical studies, see, for example, recent comprehensive reviews [37, 38].

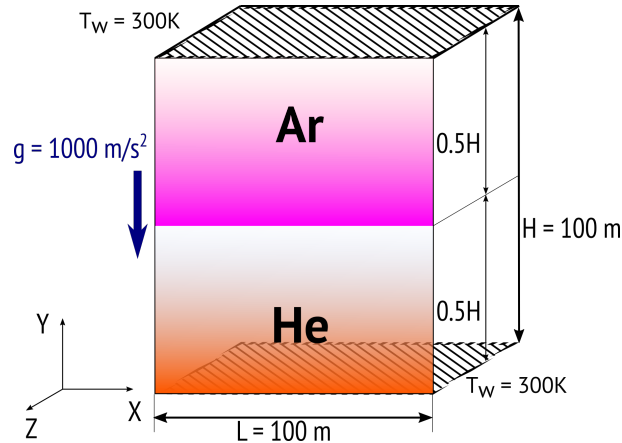


**Figure 5.** Rayleigh–Taylor instability. General scheme and computational domain geometry

We simulated numerically the RT instability developing in a rarefied Ar/He mixture in 2D and 3D formulations using the SMILE++ and HyCFS-R codes to assess the effects of rarefaction and non-equilibrium. A sketch of domain and general problem setup are shown in Fig. 5. A two-layer system consisting of argon layer over a helium layer in a gravitational field is simulated. The interface between gases at the initial moment of time is parallel to the  $X$  axis. Densities and pressures on both sides of the interface are distributed at the initial moment in accordance with barometric formulas.

The size of the computational domain is  $100 \times 100$  m, the mean free paths in gases at the interface are  $\lambda_{\text{He}} = 2.8 \times 10^{-2}$  and  $\lambda_{\text{Ar}} = 8.8 \times 10^{-3}$  m, and the densities are  $\rho_{\text{He}} = 10^{-6}$  and  $\rho_{\text{Ar}} = 10^{-5}$  kg/m<sup>3</sup>, respectively. The pressure at the interface is  $p = 0.62$  Pa. If the wavelength

of emerging disturbances (see below) is taken as a flow characteristic scale, then the Knudsen number is  $\text{Kn} = 3.6 \cdot 10^{-3}$ .

In order to reduce the difference between the characteristic time of instability development and the characteristic molecular times, the acceleration of gravity  $g$  is increased to  $1000 \text{ m/s}^2$ . The Atwood number  $\text{At} = (\rho_1 - \rho_2)/(\rho_1 + \rho_2)$  of the problem is equal to  $9/11$ .

The DSMC computations are carried out using up to 60 million model particles, time step is equal to  $4 \times 10^{-6} \text{ s}$ , the flow macroparameters are averaged over 1000 time steps for total of 2 million time steps. The continuum computations are performed on a grid consisting of up to 8 million cells using 2nd order TVD scheme and 2nd order explicit RK TVD time integration scheme.

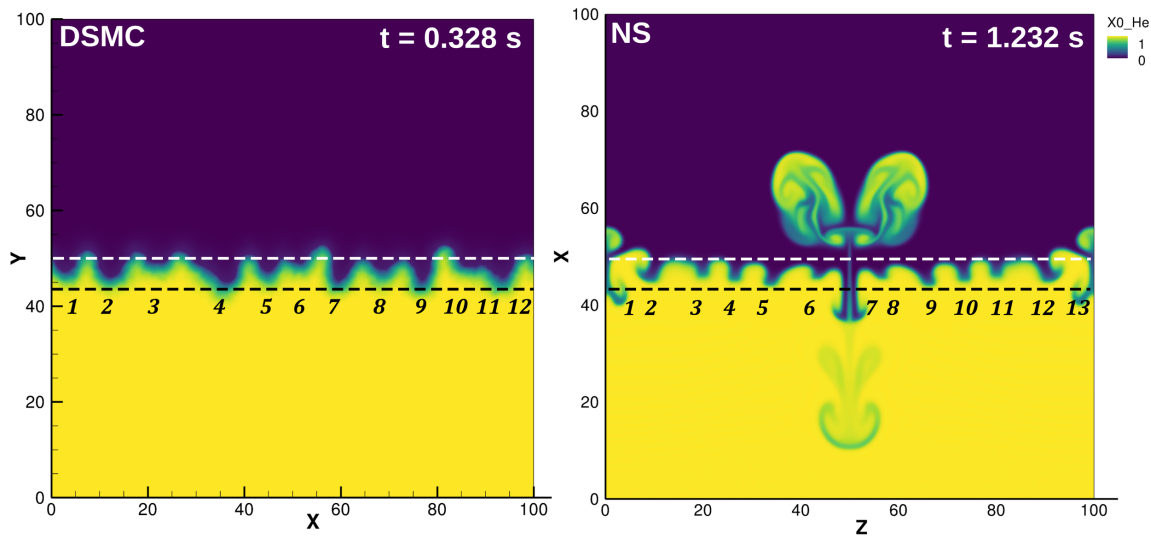


**Figure 6.** Comparison of He molar fraction in DSMC and NS computations

Because of different types of disturbances used for initial flow forcing in kinetic and continuum computations, the instabilities emerge in slightly different ways and at different rates. However, qualitative analysis shows that at the early stage of the instability development both approaches predict similar wavelengths of emerging disturbances although at different time instants. In Fig. 6 the molar fraction of helium is presented for both simulations. The white dashed line indicates the original position of the Ar/He interface, and the black dashed line shows the maximum amplitude of the spikes. As can be seen, the numbers of spikes are similar and their shapes are roughly the same. So it seems that in both cases, instability waves corresponding to the same fastest growing frequency develop from a wide spectrum of superposed disturbances. In the DSMC computation, the spikes are considerably less uniform than in the continuum simulation because the DSMC method induces a high level of the macroparameters fluctuations as mentioned above.

## 2.4. Richtmyer–Meshkov Instability

The Richtmyer–Meshkov (RM) instability develops when lighter and heavier fluids separated by a contact surface are impulsively accelerated by a passing shock wave. It can be considered as a Rayleigh–Taylor instability with the gravity force replaced by an inertial force acting during a small time interval. This instability is important in astrophysics, controlled thermonuclear fusion, supersonic combustion and many other areas [39].

Numerical simulations of the RM instability are performed by solving the BGK model kinetic equation, by using the DSMC method and on the basis of the Navier–Stokes equations. The Mach number of the incident shock  $M_s$  is varied from 1.5 to 8, the density ratio across the contact surface  $\rho_2/\rho_1$  – from 2 to 10. The rarefaction degree is determined by the value of the Reynolds number  $Re$  based on the wavelength of a sinusoidal perturbation imposed on the contact surface at the initial moment or by the corresponding value of the Knudsen number  $Kn$ . The Reynolds number is varied from 50 to infinity (in an inviscid continuum computation).

A typical pattern of the RM instability development is shown in Fig. 7 where the results of a BGK simulation performed for a monatomic gas are presented. The computational grid contains  $1200 \times 300$  points in the physical space and  $33 \times 33$  points in the velocity space.

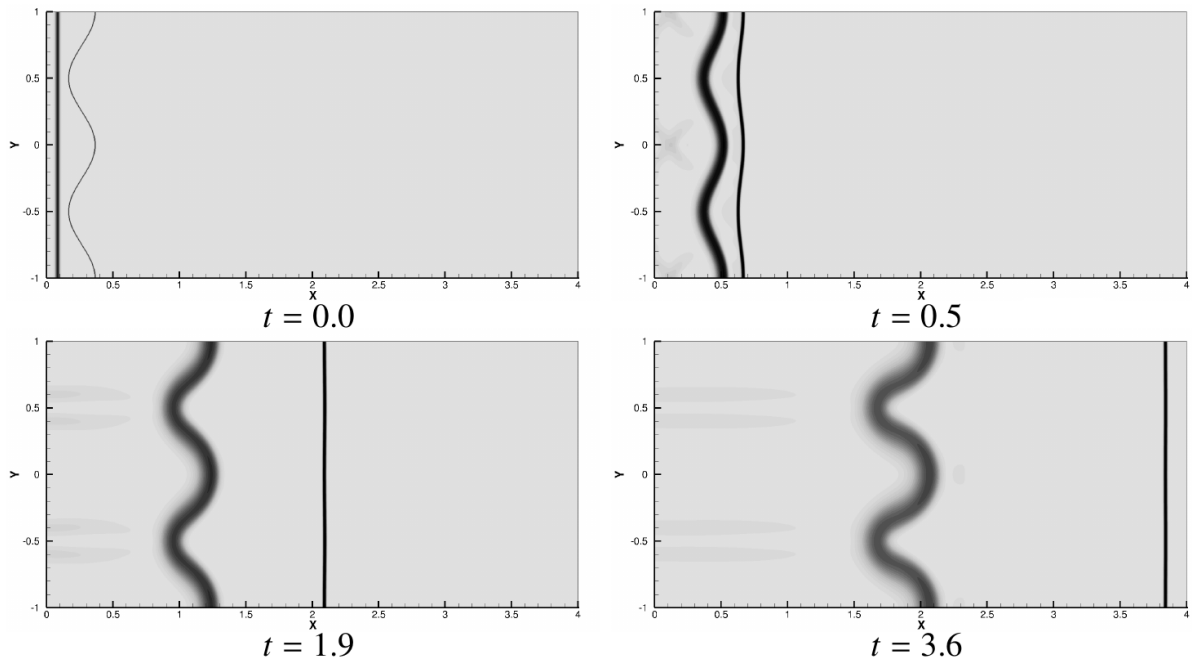


**Figure 7.** Richtmyer–Meshkov instability development in kinetic simulation at  $M_s = 1.5$ ,  $\rho_2/\rho_1 = 2$ ,  $Re = 400$ ,  $Kn = 0.041$ . Density gradient flowfields

As a result of the interaction with the passing shock wave, the contact surface begins to move in the same direction. Simultaneously, the amplitude of the contact surface perturbation, which is measured as a distance  $\Delta x_c$  between developing “bubbles” and “spikes”, starts growing. At high Reynolds numbers, the secondary KH instability arises on the distorted contact surface and the lighter and heavier gases are effectively mixed by emerging small-scale pulsations.

The results of kinetic simulations are in close agreement with each other. It can be seen in Fig. 8 where numerical flowfields at the same time moment are compared. The largest deviation of the molecular distribution function in the kinetic simulations from the equilibrium function is predictably observed inside the shock wave.

The instability grows significantly faster at higher Mach numbers of the incident shock wave. A higher density ratio across the contact surface also promotes the development of the RM instability. As can be expected, the growth of perturbations is suppressed by rarefaction effects. At lower Reynolds numbers (larger Knudsen numbers) the interface between two gases is smeared and the secondary instability does not develop. Moreover, at the lowest of the Reynolds

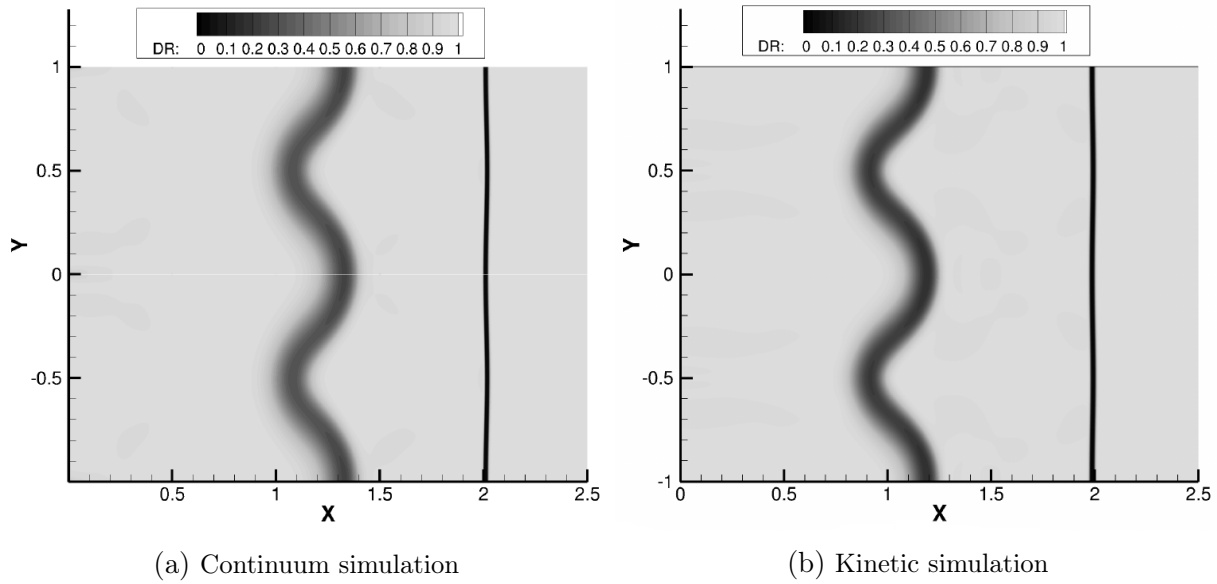


**Figure 8.** Density gradient flowfields in continuum (a) and kinetic (b) simulations at  $M_s = 1.5$ ,  $\rho_2/\rho_1 = 2$ ,  $Re = 400$ ,  $Kn = 0.041$

numbers studied,  $Re = 50$ , the distance between spikes and bubbles stops growing after some time, see Fig. 9.

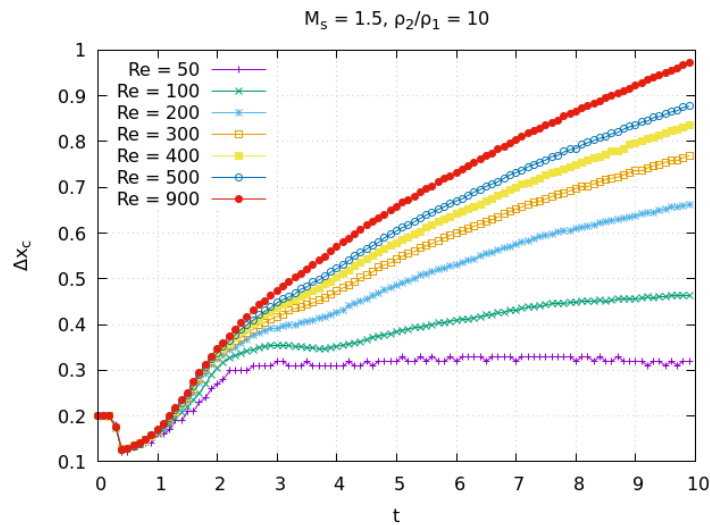


**Figure 9.** Growth of amplitude of contact surface perturbation at various Reynolds numbers.  $M_s = 1.5$ ,  $\rho_2/\rho_1 = 10$

## Conclusion

Statistical and deterministic numerical methods for solving the kinetic equations currently reached a level, at which it is possible to use them for numerical simulation of complex unsteady flows associated with the emergence of hydrodynamic instabilities. The numerical simulations can be performed now using a typical laboratory-level computational cluster, especially if it is equipped with modern GPU hardware. In the presented results of computations based on the kinetic approach the development of instabilities emerging in free shear flows or induced by external body forces has been successfully reproduced. Good agreement is observed between

kinetic and continuum approaches when continuum simulations are also performed. The most interesting results are obtained using the DSMC method, because the statistical fluctuations inherent to the method lead to scenarios of the instability development similar to the one observed in experiments.

## Acknowledgements

This work was supported by the Russian Science Foundation, grant No. 23-11-00258.

*This paper is distributed under the terms of the Creative Commons Attribution-Non Commercial 3.0 License which permits non-commercial use, reproduction and distribution of the work without further permission provided the original work is properly cited.*

## References

1. Rapaport, D.C.: Molecular-dynamics study of Rayleigh–Bénard convection. *Phys. Rev. Lett.* 60(24), 2480–2483 (1988). <https://doi.org/10.1103/physrevlett.60.2480>
2. Puhl, A., Malek Mansour, M., Marechal, M.: Quantitative comparison of molecular dynamics with hydrodynamics in Rayleigh–Bénard convection. *Phys. Rev. A* 40(4), 1999–2012 (1989). <https://doi.org/10.1103/PhysRevA.40.1999>
3. Stefanov, S., Cercignani, C.: Monte Carlo simulation of Bénard’s instability in a rarefied gas. *Eur. J. Mech. B/Fluids* 11(5), 543–554 (1992).
4. Golshtein, E., Elperin, T.: Convective instabilities in rarefied gases by Direct Simulation Monte Carlo method. *J. Thermophys. Heat Transfer* 10(2), 250–256 (1996). <https://doi.org/10.2514/3.782>
5. Stefanov, S., Cercignani, C.: Monte Carlo simulation of the Taylor–Couette flow of a rarefied gas. *J. Fluid Mech.* 256, 199–213 (1993). <https://doi.org/10.1017/S0022112093002769>
6. Reichelman, D., Nanbu, K.: Monte Carlo direct simulation of the Taylor instability in a rarefied gas. *Phys. Fluids A* 5, 2585–2587 (1993). <https://doi.org/10.1063/1.858775>
7. Hirshfeld, D., Rapaport, D.C.: Molecular dynamics simulation of Taylor–Couette vortex formation. *Phys. Rev. Lett.* 80(24), 5337–5340 (1998). <https://doi.org/10.1103/PhysRevLett.80.5337>
8. Aristov, V.V., Zabelok, S.A.: Vortex structure of the unstable jet studied on the basis of the Boltzmann equation. *Matem. Modelirovanie* 13(6), 87–92 (2001, in Russian).
9. Rovenskaya, O.I., Aristov, V.V., Farkhutdinov, T.I.: Investigation of the Taylor–Görtler instability in jets with help of kinetic approach. *Matematika i Matem. Modelirovanie* 01, 38–54 (2016, in Russian). <https://doi.org/10.7463/mathm.0116.0833621>
10. Yang, J.-Y., Chang, J.-W.: Rarefied flow instability simulation using model Boltzmann equations. *AIAA Paper No. 97-2017* (1997). <https://doi.org/10.2514/6.1997-2017>
11. Kadau, K., Germann, T.C., Hadjiconstantinou, N.G., *et al.*: Nanohydrodynamics simulations: an atomistic view of the Rayleigh–Taylor instability. *Proc. Nat. Acad. Sci.* 101(6), 5851–5855 (2004). <https://doi.org/10.1073/pnas.0401228101>

12. Kadau, K., Barber, J.L., Germann, T.C, *et al.*: Atomistic methods in fluid simulation. *Phil. Trans. R. Soc. A* (368), 1547–1560 (2010). <https://doi.org/10.1098/rsta.2009.0218>
13. Gallis, M.A., Koehler, T.P., Torczynski, J.R., Plimpton, S.J.: Direct simulation Monte Carlo investigation of the Richtmyer–Meshkov instability. *Phys. Fluids* 27(8), 084105 (2015). <https://doi.org/10.1063/1.4928338>
14. Gallis, M.A., Koehler, T.P., Torczynski, J.R., Plimpton, S.J.: Direct simulation Monte Carlo investigation of the Rayleigh–Taylor instability. *Phys. Rev. Fluids* 1(4), 043403 (2016). <https://doi.org/10.1103/PhysRevFluids.1.043403>
15. Kudryavtsev, A.N., Kashkovsky, A.V., Shershnev, A.A.: Investigation of Kelvin–Helmholtz instability with the DSMC method. *AIP Conf. Proc.* 2125, 030028 (2019). <https://doi.org/10.1063/1.5117410>
16. Kashkovsky, A.V., Kudryavtsev, A.N., Shershnev, A.A.: Numerical simulation of the Rayleigh–Taylor instability in rarefied Ar/He mixture using the Direct Simulation Monte Carlo method. *J. Phys. Conf. Ser.* 1382, 012154 (2019). <https://doi.org/10.1088/1742-6596/1382/1/012154>
17. Kashkovsky, A.V., Kudryavtsev, A.N., Shershnev, A.A.: Direct Monte Carlo simulation of development of the Richtmyer–Meshkov on the Ar/He interface. *J. Phys. Conf. Ser.* 1404, 012109 (2019). <https://doi.org/10.1088/1742-6596/1404/1/012109>
18. Kashkovsky, A.V., Kudryavtsev, A.N., Shershnev, A.A.: DSMC simulation of instability of plane supersonic jet in coflow. *AIP Conf. Proceedings* 2504, 030087 (2023). <https://doi.org/10.1063/5.0132264>
19. Kashkovsky, A.V., Kudryavtsev, A.N., Shershnev, A.A.: Numerical simulation of the Rayleigh–Taylor instability in rarefied mixture of monatomic gases using continuum and kinetic approaches. *AIP Conf. Proceedings* 2504, 030111 (2023). <https://doi.org/10.1063/5.0132266>
20. Kudryavtsev, A.N., Epstein, D.B.: Richtmyer–Meshkov instability in a rarefied gas, results of continuum and kinetic numerical simulations. *AIP Conf. Proceedings* 2125, 020010 (2019). <https://doi.org/10.1063/1.5117370>
21. Kudryavtsev, A.N., Poleshkin, S.O., Shershnev, A.A.: Numerical simulation of the instability development in a compressible mixing layer using kinetic and continuum approaches. *AIP Conf. Proc.* 2125, 030033 (2019). <https://doi.org/10.1063/1.5117415>
22. Poleshkin, S.O., Kudryavtsev, A.N.: Kinetic simulation of the Rayleigh–Taylor instability. *AIP Conf. Proc.* 2288, 030010 (2020). <https://doi.org/10.1063/5.0028881>
23. Malkov, E.A., Kudryavtsev, A.N.: Non-stationary Antonov self-gravitating layer. *MNRAS* 491(3), 3952–3966 (2020). <https://doi.org/10.1093/mnras/stz3276>
24. Ivanov, M.S., Kashkovsky, A.V., Vashchenkov, P.V., Bondar, Ye.A.: Parallel object-oriented software system for DSMC modeling of high-altitude aerothermodynamic problems. *AIP Conf. Proceedings* 1333, 211–218 (2011). <https://doi.org/10.1063/1.3562650>
25. Kashkovsky, A.V.: 3D DSMC computations on a heterogeneous CPU-GPU cluster with a large number of GPUs. *AIP Conf. Proceedings* 1628(1), 192–198 (2014) <https://doi.org/10.1063/1.4902592>

26. Malkov, E.A., Bondar, Ye.A., Kokhanchik, A.A., *et al.*: High-accuracy deterministic solution of the Boltzmann equation for the shock wave structure. *Shock Waves* 25(4), 387–397 (2015). <https://doi.org/10.1007/s00193-015-0563-6>
27. Malkov, E.A., Poleshkin, S.O., Kudryavtsev, A.N., Shershnev, A.A.: Numerical approach for solving kinetic equations in two-dimensional case on hybrid computational clusters. *AIP Conf. Proceedings* 1770, 030077 (2016). <https://doi.org/10.1063/1.4964019>
28. Bhanthnagar, P.L., Gross, E.P., Krook, M.: A model for collision processes in gases. I. Small amplitude processes in charged and neutral one-component systems. *Phys. Rev.* 94(3), 511–525 (1954). <https://doi.org/10.1103/PhysRev.94.511>
29. Holway, L.H.: New statistical models for kinetic theory: methods of construction. *Phys. Fluids* 9(9), 1658–1673 (1966). <http://doi.org/10.1063/1.1761920>
30. Shakhov, E.M.: Approximate kinetic equations in rarefied gas theory. *Fluid Dynamics* 3(1), 112–115 (1968). <http://doi.org/10.1007/BF01016254>
31. Kudryavtsev, A.N., Shershnev, A.A.: Numerical simulation of microflows using direct solving of kinetic equations with WENO schemes. *J. Sci. Comp.* 57(1), 42–73 (2013). <http://doi.org/10.1007/s10915-013-9694-z>
32. Shershnev, A.A., Kudryavtsev, A.N., Kashkovsky, A.V., *et al.*: A numerical code for a wide range of compressible flows on hybrid computational architectures. *Supercomputing Frontiers and Innovations* 9(4), 85–99 (2022). <https://doi.org/10.14529/jsfi220408>
33. Ho, C.-M., Huerre, P.: Perturbed free shear layers. *Ann. Rev. Fluid Mech.* 16, 365–424 (1984). <https://doi.org/10.1146/annurev.fl.16.010184.002053>
34. Kashkovsky, A.V., Kudryavtsev, A.N., Shershnev, A.A.: Development of compressible mixing layer instability simulated using the Direct Simulation Monte Carlo method. *Supercomputing Frontiers and Innovations* 11(2), 48–64 (2024). <https://doi.org/10.14529/jsfi240204>
35. Kelly, R.E.: On the stability of an inviscid shear layer which is periodic in space and time. *J. Fluid Mech.* 27(4), 657–689 (1967). <https://doi.org/10.1017/S0022112067002538>
36. Watanabe, D., Maekawa, H.: Transition of supersonic plane jet due to symmetric/antisymmetric unstable modes. *J. Turbulence* 3, 047 (2002). <https://doi.org/10.1088/1468-5248/3/1/047>
37. Zhou, Y.: Rayleigh–Taylor and Richtmyer–Meshkov instability induced flow, turbulence, and mixing. I. *Phys. Rep.* 720–722, 1–136 (2017). <https://doi.org/10.1016/j.physrep.2017.07.005>
38. Zhou, Y.: Rayleigh–Taylor and Richtmyer–Meshkov instability induced flow, turbulence, and mixing. II. *Phys. Rep.* 723–725, 1–160 (2017). <https://doi.org/10.1016/j.physrep.2017.07.008>
39. Brouillette, M.: The Richtmyer–Meshkov instability. *Ann. Rev. Fluid Mech.* 34, 445–468 (2002). <https://doi.org/10.1146/annurev.fluid.34.090101.162238>